ULTRAVIOLET LIGHT ASSISTED SYNTHESIS OF MAGNETOPLASMONIC NANOPARTICLES

C. IACOVITA[a], G. STIUFIUC[b], A. FLOREA[c], R. STIUFIUC[a*],
C. M. LUCACIU[a]

[a] *Department of Pharmaceutical Physics-Biophysics, "Iuliu Hatieganu"
University of Medicine and Pharmacy, L. Pasteur 6, 400349 Cluj-Napoca,
Romania.*
[b] *Faculty of Physics, ''Babes-Bolyai'' University, Kogalniceanu 1,400084, Cluj-
Napoca, Romania*
[c] *Department of Cell and Molecular Biology, ''Iuliu Hatieganu'' University of
Medicine and Pharmacy, L. Pasteur 6, 400349 Cluj-Napoca, Romania.*

We report a new photochemical method to produce water-dispersible core-shell iron-oxide-gold nanoparticles (Fe_3O_4@Au NPs). The Fe_3O_4 magnetic nanoparticles (MNPs) prepared by using the oleic acid/oleylamine method, hydrophylized with tetramethylammonium hydroxide were capped with citrate anions. Gold coating was achieved by UV irradiation of Fe_3O_4 MNPs suspended in Au^{3+} solution. UV-VIS absorption spectra revealed the existence of a strong plasmonic peak, attributed to the Au shell, which red-shifts as a function of the shell thickness surrounding the magnetic core. TEM images revealed the presence of magneto-plasmonic NPs with core-shell architecture of different geometries. The plasmonic properties of the NPs have been evaluated by means of Surface Enhanced Raman Spectroscopy. The SER spectra of methylene blue (MB) obtained using the here reported magneto-plasmonic NPs as Raman substrates are very similar with those obtained using "classical" Ag and Au colloids.

1. Introduction

The development of core-shell nanoparticles (NPs) simultaneously possessing plasmonic and magnetic properties in a so-called magneto-plasmonic nanostructure is of a particularly interest for biomedical use [1]. The magnetic properties of the core make them ideal candidates for enhanced magnetic resonance imaging, biological separation, magnetic drug delivery or magnetic hyperthermia applications [2, 3]. A major obstacle limiting the applicability of magnetic NPs in biological applications is the lack of surface tunability. Gold coating can overcome this obstacle, owing to the surface chemistry and biological reactivity of gold [4], and can provide additional plasmonic properties. One of the most important functionalities associated with the existence of a gold shell is represented by the occurrence of localized surface plasmons [5]. Moreover, gold's chemically inert surface can be functionalized for different purposes: enhanced solubility in various media, improved biocompatibility and subsequent attachment of various biomolecules such as proteins and nucleic acids [6].

Previous studies concerning magneto plasmonic nanoparticles (MNPs) have been focused on using as core materials iron oxides nanoparticles (magnetite or maghemite) because these materials exhibit high magnetic susceptibilities and very low toxicity [7]. Several methods for the

---

*Corresponding author: rares.stiufiuc@umfcluj.ro

synthesis of gold-coated magnetic particles have been reported, including gamma-ray radiation, laser ablation, sonochemical reaction, layer-by-layer electrostatic deposition, chemical reduction, and micelle methods [1]. The main challenge is to control the size and shape of these hybrid structures. In general, the engineering of magneto-plasmonic NPs has been done in two steps. Several studies have been focused on the deposition of a thin gold layer onto the outer surface of MNPs in organic solvent, followed by their transfer in aqueous solution [8-10]. Alternatively, prior to the deposition of Au shell, the magnetic cores have been transferred from organic solvent into water [11-13]. In other studies, the surface of MNPs has been firstly decorated with Au seeds, and subsequently, by iterative processes, Au ions have been systematically reduced in order to grow an Au shell around MNPs [12, 14-16]. However, attaining a uniform and continuous Au layer still remain a great challenge.

In this paper we present a novel two-stage synthesis method of magneto-plasmonic NPs. Firstly, the hydrophobic Fe_3O_4 MNPs are transfer into water phase and capped with citrate groups and then, under ultraviolet illumination, the Au ions are reduced preferentially on the citrate capped Fe_3O_4 MNPs generating the formation of an Au nanoshell surrounding the magnetic core. UV-VIS absorption spectroscopy is used to detect the plasmon resonance peak of gold on the surface of MNPs, while transmission electron microscopy (TEM) was employed to study the morphology of the Au coated Fe_3O_4 NPs. The plasmonic properties of the as-synthesized hybrid $Fe_3O_4@Au$ nanoparticles have been evaluated by means of Surface Enhanced Raman Spectroscopy (SER) using methylene blue as analyte.

2. Materials and methods.

2.1 Material

All reagents used were of analytical grade. Iron (III) acetylacetonate $(Fe(acac)_3)$, tetramethylammonium hydroxide (TMAOH), hexane, toluene and ethanol were purchased from Merck. Oleic acid, oleylamine and octylether were purchased from Sigma-Aldrich, while tri-natriumcitrate-dihydrate, and tetrachloroauric(III) acid trihydrate $(HAuCl_4)$ were from Roth. All reagents were used without further purification. Ultrapure water (18.2 MO, Barnstead EASYPure ROdi) was used for the preparation of aqueous solutions.

2.2 Preparation of Magnetic Nanoparticles and Colloids

In a general synthetic procedure for the preparation of Fe_3O_4 MNPs 2 mmol of $Fe(acac)_3$ (0.7 g) were dissolved in a mixture of 5 mmol of acid oleic (OA) (1,6 ml), 8 mmol of oleylamine (OY) (2,6 ml) and 4,3 mmol of octylether (1,3 ml). The solution was stirred thoroughly at room temperature for 10 minutes then transferred in sealed glass bottles and heated at 300˚C for 1h. The glass bottle was let to cool at room temperature and the obtained black precipitates were washed several times with ethanol, separated by using permanent magnets, dispersed and kept in 10 ml of ethanol. The Au and Ag colloids were prepared by the classic gold and silver ions reduction using citrate and hydroxylamine, respectively, as described elsewhere [20].

2.3. Methods and instrumentation

The UV–VIS absorption spectra were recorded with a T92+ UV–VIS Spectrophotometer from PG INSTRUMENTS, using standard quartz cells at room temperature, over a spectral range between 350 nm and 900 nm, with a spectral resolution of 2 nm. TEM images were taken on a Jeol JEM 1010 transmission electron microscope (Jeol Ltd., Tokyo, Japan), equipped with a Mega VIEW III camera (Olympus, Soft Imaging System, Münster, Germany), operating at 80 kV. The TEM samples were prepared by deposition of 5 µl drops of each solution on carbon-coated copper grids. DLS and Zeta (ξ) potential measurements were taken by using a Zetasizer Nano ZS90 (Malvern Instruments, Worcestershire, UK) in a 90° configuration. All SER spectra have been recorded in 1 ml glass vials filled with 540 ml of colloid and 60 ml of the analyte, in back-scattering geometry and in the 200–2000 cm^{-1} range, using a DeltaNu Advantage spectrometer (DeltaNu, Laramie, WY) equipped with a laser diode emitting at 785 nm. The laser power was 100 mW and the spectral

resolution was 5 cm^{-1}. Each SER spectrum is the average of 10 recordings taken with an acquisition time of 20 seconds.

3. Results and discussions

Oleic acid (OA) and oleylamine (OY) in the presence of octylether gave rise to spherical Fe$_3$O$_4$ MNPs (figure 1) [17]. According to the size distribution histogram (figure 1), the Fe$_3$O$_4$ MNPs are monodispersed with a mean diameter situated around 12.4 nm. DLS measurement of Fe$_3$O$_4$ MNPs dispersed in toluene exhibits a dominant peak centered at 24.4 nm (figure 2a). The difference of 12 nm is attributed to OA-OY monolayer existing on MNPs surface, which is not visible in the TEM images. For NPs coated with organic layer the hydrodynamic diameter provided by DLS measurements is usually greater to that obtained from TEM measurements as it was previously reported [18].
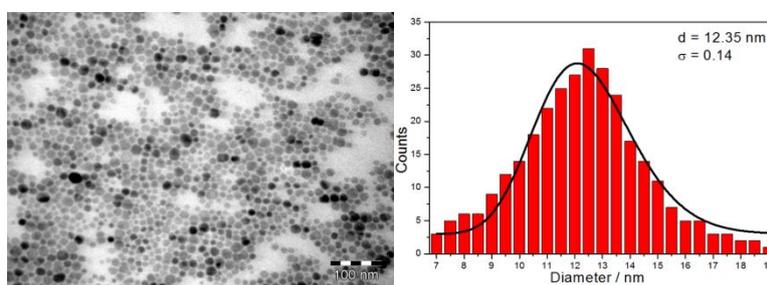

Fig.1 TEM image of Fe$_3$O$_4$ nanoparticles capped with oleic acid and oleylamine (left) and its corresponding size distribution histogram (right) fitted to a log-normal distribution (black line)

The second peak around 300 nm present in DLS measurement (figure 2a) can be attributed to the existence of aggregates of Fe$_3$O$_4$ MNPs. Since the first peak in the size distribution has a higher intensity than the second one (figure 2a) and based on the fact that an aggregate scatters much more light than an individual NP (the scattered light is proportional to the sixth power of NP's diameter), one can conclude that individual spherical OA-OY capped Fe$_3$O$_4$ are dominant as it can be also observed in the TEM image (figure 1). These individual MNPs will serve as cores for a further growth of gold shell around them.
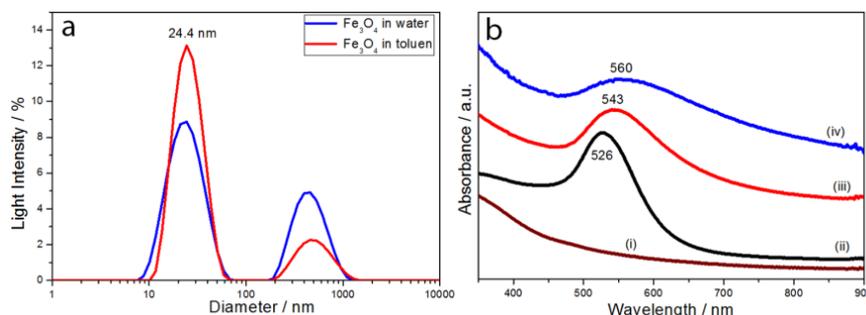

Fig. 2. (a) Hydrodynamic size of Fe3O4 nanoparticles dispersed in toluene and water, (b) UV-VIS absorption spectra of Fe3O4 (i), citrate capped AuNPs (ii) and Fe3O4@Au nanoparticles (iii) and (iv)

The MNPs dispersed in a volume of 0.5 ml ethanol, taken from the stock solution (10 ml), were collected with a magnet and washed several times with 4 ml of 25% (w/w) TMAOH aqueous solution followed by 15 minutes of ultrasonication. Afterwards, the Fe$_3$O$_4$ MNPs have been washed

with ethanol and redispersed in 2 ml of water. The water soluble MNPs have a zeta potential of -43,7 mV, indicating that the negatively charged OH groups replaced OA-OY molecules at the Fe_3O_4 surface [11]. The characteristic peak of individual Fe_3O_4 MNPs in DLS spectrum (blue spectrum in figure 2a) is located at the same position (24.4 nm) as for those dispersed in toluene, indicating that the hydrophilized MNPs have the same hydrodynamic radius.

Prior to the deposition of Au layer onto the surface of water soluble Fe_3O_4 MNPs, they were washed several times with 25% (w/w) sodium citrate aqueous solutions, in order to replace the OH groups with citrate groups. Afterwards, the Fe_3O_4 MNPs were redispersed in 2 ml of 1 % (w/w) sodium citrate aqueous solution and used for gold deposition. This was achieved by mixing 1 ml citrate capped MNPs with 4 ml of aqueous solution of $HAuCl_4$ (10^{-2} M) followed by a 5 minutes exposition to an ultraviolet (UV) lamp (Vilber Lourmat, 6W, $\lambda = 254$ nm). The UV-VIS spectra of the Fe3O4@Au NPs show a distinct band centred at 543 nm characteristic of the surface plasmon band of AuNPs [8,10,11]. This band is not present neither in the UV-VIS spectra of water-soluble Fe_3O_4 MNPs nor in that of citrate capped AuNPs (figure 2b). The Fe_3O_4 MNPs show no measurable features in the visible range [8,10,11], while the Au NPs, prepared by exposing a mixture containing 1 ml of citrate 1% aqueous solutions and 4 ml of $HAuCl_4$ (10^{-2} M) aqueous solution to a UV radiation in the same conditions display a surface plasmon resonance band at 526 nm (figure 2b). The absorption band of Fe3O4@Au NPs is broaden (curve (iii) in figure 2b), indicating a thickness polidispersivity of the gold coatings. The absorption band red-shifts to 560 nm and became more broaden (curve (iv) in figure 2b), if the amount of $HAuCl_4$ aqueous solution in the solution mixture is increased to 8 ml, suggesting that the gold thickness around Fe_3O_4 MNPs is increased [8,10,11].
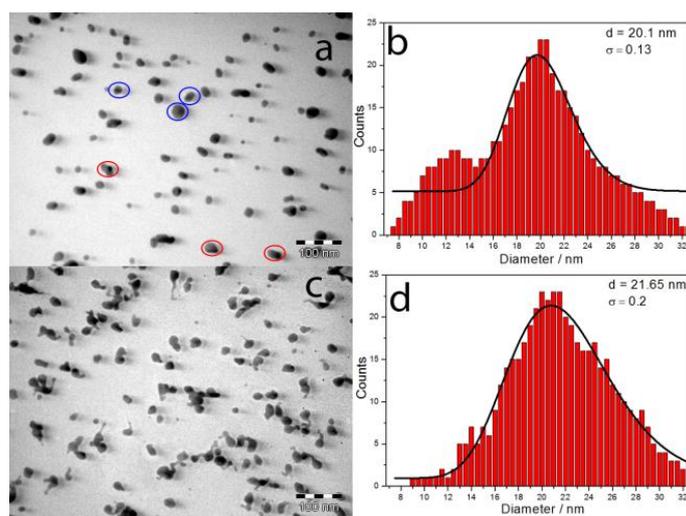

Fig.3. TEM images of Fe3O4@Au NPs (a) and (c) and their corresponding size distribution histogram (b) and (d) fitted to a log-normal distribution (black line)

TEM analysis of Fe3O4@Au NPs reveals that the average inorganic diameter increases from 12.4 nm, in the case of Fe_3O_4 MNPs, to 20.1 nm for hybrid Fe3O4@Au NPs (figure 3b). At a closer inspection of the TEM image (figure 3a) three types of NPs are detected. One can clearly observe the existence of Fe3O4@Au NPs with a core-shell architecture (blue circles in figure 3a). The Au shell is not uniformly distributed around the spherical magnetic core, as can be judged from the contrast variation between the dark Fe_3O_4 core and the lighter Au shell [10]. In the case of other nanoparticles the magnetic core is not fully covered by an Au shell (red circles in figure 3a); the Au forms solid NPs incorporating a certain area of the spherical surface of Fe_3O_4. Small NPs associated with the shoulder in the histogram (figure 3b) are also visible. They can be either free Fe_3O_4 NPs or small Au NPs formed separately from magnetic core. Their number is significantly reduced when the amount of gold is doubled in the reaction solution (figure 3d). In this case the average diameter increases to 21.7 nm (figure 3d) and Fe3O4@Au NPs displaying a core-shell architecture are predominant in the TEM image (figure 3c).
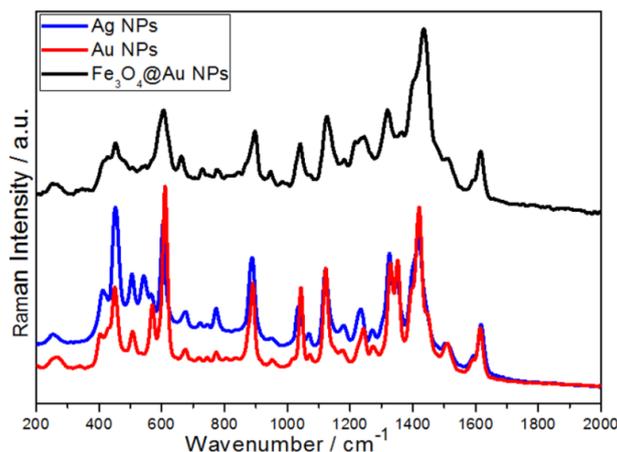
Fig. 4. SER spectra of methylene blue (10^{-5} M) acquired on Fe3O4@Au NPs, hydroxylamine reduced Ag and citrate capped Au colloids using 785 nm excitation wavelength. The spectra are normalized and vertically shifted for clarity.

Further biomedical applications of the as-produced Fe_3O_4@Au NPs require the assessment of their plasmonic properties. Figure 4 displays the SER spectra of methylene blue, used as test analyte, acquired on Ag, Au and Fe_3O_4@Au NPs. Prior to the SERS recordings the Fe_3O_4@Au NPs were magnetically separated with a strong neodymium magnet for isolating them from any purely gold nanoparticles which were eventually formed during the photochemical reduction process. The characteristic vibrational bands of methylene blue [19] are clearly visible being similar with those provided by hydroxylamine-reduced Ag and citrate reduced Au colloids, which were chosen as a reference. Based on this observation one clearly conclude that the as-synthesized hybrid NPs possess plasmonic properties similar with those of "classical" noble metal colloids.

4. Conclusions

A facile method to synthesize magneto-plasmonic NPs has been described, together with their morphological and optical characterization. The magneto-plasmonic NPs have been successfully synthesized by firstly converting hydrophobic magnetic nanoparticles into hydrophilic ones, capping them with citrate molecules and deposition of an Au plasmonic shell onto the outer surface of the magnetic cores through the reduction of Au ions by citrate molecules under ultraviolet illumination. The UV-VIS spectroscopy indicated that the magneto-plasmonic NPs exhibit a plasmon resonant band dependent on Au shell thickness. Further morphological TEM examination reveals the presence of magneto-plasmonic NPs exhibiting a core-shell architecture. The as-synthesized magneto-plasmonic NPs possess plasmonic properties similar with those of gold and silver nanoparticles, allowing the recording of the SER spectra of methylene blue.

References

[1] H. Zhou, F. Zou, K. Koh, J. Lee, Journal of Biomedical Nanotechnology, **10**, 2921 (2014).

[2] N. Tran, T. J. Webster, Journal of Material Chemistry, **20**, 8760 (2010).

[3] T. D. Schladt, K. Schneider, H. Schildb, W. Tremel, Dalton Transactions, **40**, 6315 (2011).

[4] I. Urries, C. Muñoz, L. Gomez, C. Marquina, V. Sebastian, M. Arruebo, J. Santamaria, Nanoscale, **6(15)**, 9230(2014)

[5] X. Huanga, and M. A. El-Sayeda, Journal of Advanced Research, **1**, 13 (2010).

[6] E. C. Dreaden, A. M. Alkilany, X. Huang, C. J. Murphy and M. A. El-Sayed, Chemical Society Reviews, **41**, 2740 (2012).

[7] W. Wu, Z. Wu, T. Yu, C. Jiang and W.-S. Kim, Sci. Technol. Adv. Mater., **16,** 023501(2015).

[8] Z. Xu, Y. Hou and S. Sun, JACS, **129**, 8698 (2007).

[9] S. Pal, M. Morales, P. Mukherjee and Hariharan Srikanth, Journal of Applied Physics, **105**, 07B504 (2009).

[10] I. Robinson, Le D. Tung, S. Maenosono, C. Walti and N. T. K. Thanh, Nanoscale, **2**, 2624 (2010).

[11] J. K. Lim, R. D. Tilton, A. Eggeman and S. A. Majetich, Journal of Magnetism and Magnetic Materials, **311**, 78 (2007).

[12] C. S. Levin *et al.*, ACS Nano, **3**, 1379 (2009).

[13] E. D. Smolensky *et al.*, Chem. Commun., **47**, 2149 (2011).

[14] J. L. Lyon *et al.*, Nano Lett., **4**, 719 (2004).

[15] I. Y. Goon *et al.*, Chem. Mater. **21**, 673 (2009).

[16] J. Ren *et al.*, Chem. Commun., 47, 11692 (2011).

[17] Sh. Sun *et al.*, JACS, **126(1)**, 273 (2004).

[18] R. Stiufiuc *et al.*, Journal of Nanomaterials, 2013, 1(2013).

[19] S. D. Roy, M. Ghoshb and J. Chowdhurya, J. Raman Spectrosc., **46**, 451 (2015).

[20] R. Stiufiuc *et al.*, Phys.Chem.Chem.Phys., **17**, 1281 (2015).